Article No. jmbi.1999.3459 available online at http://www.idealibrary.com on IDEAL® J. Mol. Biol. (2000) 296, 311–321

JMB

Stator Structure and Subunit Composition of the V_1/V_0 Na^+-ATPase of the Thermophilic Bacterium *Caloramator fervidus*

Trees Ubbink-Kok[1], Egbert J. Boekema[2], Jan F. L. van Breemen[2], Alain Brisson[2], Wil N. Konings[1] and Juke S. Lolkema[1]*

[1]*Department of Microbiology Groningen Biomolecular Sciences and Biotechnology Institute, University of Groningen, Kerklaan, 9751 NN Haren, The Netherlands*

[2]*Department of Biophysical Chemistry, Groningen Biomolecular Sciences and Biotechnology Institute University of Groningen Nijenborgh 4, Groningen The Netherlands*

**Corresponding author*

The V-type Na^+-ATPase of the thermophilic, anaerobic bacterium *Caloramator fervidus* was purified to homogeneity. The subunit compositions of the catalytic V_1 and membrane-embedded V_0 parts were determined and the structure of the enzyme complex was studied by electron microscopy. The V_1 headpiece consists of seven subunits present in one to three copies, and the V_0 part of two subunits in a ratio of 5:2. An analysis of over 7500 single particle images obtained by electron microscopy of the purified V_1V_0 enzyme complex revealed that the stalk region, connecting the V_1 and V_0 parts, contains two peripheral stalks in addition to a central stalk. One of the two is connected to the V_0 part, while the other is connected to the first *via* a bar-like structure that is positioned just above V_0, parallel with the plane of the membrane. In projection, this bar seems to contact the central stalk. The data show that the stator structure that prevents rotation of the static part of V_0 relative to V_1 in the rotary catalysis mechanism of energy coupling in ATPases/ATPsynthases is more complex than previously thought.

Keywords: V-type ATPase; stator; rotational catalysis; Na^+-ATPase; molecular motor

Introduction

Caloramator fervidus (previously known as *Clostridium fervidus*; Collins *et al.*, 1994), originally isolated from a hot spring in New Zealand, is a strictly anaerobic bacterium that grows optimally at 68 °C (Patel *et al.*, 1987). The organism grows on amino acids and peptides that are taken up into the cell by Na^+-coupled transport systems (Speelmans *et al.*, 1989, 1993a). Bioenergetic studies have indicated that the organism does not have a proton cycle; it does not maintain an electrochemical proton gradient across the cell membrane, but, instead, a large electrochemical gradient of sodium ions is generated (Speelmans *et al.*, 1993b). As a consequence, the bacterium has no means for pH homeostasis of the cell interior and grows only in a very narrow pH range of around pH 7.

The electrochemical Na^+ gradient across the cytoplasmic membrane of *C. fervidus* is generated by an ATPase that pumps Na^+ out of the cell at the expense of ATP (Speelmans *et al.*, 1994). The enzyme complex was reconstituted in proteoliposomes and shown to be a primary Na^+ pump (Höner zu Bentrup *et al.*, 1997). The inhibitor profile of ATPase activity in solubilized membrane vesicles suggested that the *C. fervidus* Na^+-ATPase belongs to a small group of bacterial V-type ATPases (Speelmans *et al.*, 1994). Indeed, N-terminal sequencing of two subunits of the complex revealed many sequence similarities to the A and B subunits of the well-studied V-type ATPase of the mesophilic, facultative anaerobic bacterium *Enterococcus hirae* that was also shown to be a primary Na^+ pump (Takase *et al.*, 1993, 1994; Kakinuma *et al.*, 1995). V-type ATPases are normally found in the endomembranes of eukaryotes with the vacuolar H^+-ATPase of yeast as the best-known example. The third known example of a bacterial V-type ATPase is the H^+-ATPase of the aerobic thermophile *Thermus thermophilus* (Yokojama *et al.*, 1990; Tsutsumi *et al.*, 1991). In *T. thermophilus* the enzyme is believed to function as an ATP synthase, and the ability of the purified complex to synthesize ATP at the expense of the electro-

E-mail address of the corresponding author: j.s.lolkema@biol.rug.nl

0022-2836/00/60311–11 $35.00/0

chemical proton gradient was recently demonstrated (Yokojama *et al*., 1998).

V-type ATPases are believed to have a similar catalytic mechanism and structural architecture as the F-type ATP synthases that operate in oxidative phosphorylation in mitochondria and bacteria and in light-driven ATP synthesis in chloroplasts. The enzyme complexes consist of two parts, the soluble headpiece F_1/V_1 and the membrane-embedded part F_0/V_0, connected by a stalk region. Firm evidence exists that in the F-type ATP synthases, the coupling between the movement of protons through F_0 and the synthesis of ATP in F_1 is mechanical (Boyer, 1993; Abrahams *et al*., 1994; Noji *et al*., 1997; Sabbert *et al*., 1996). The free energy of the protons moving down their gradient would drive the physical rotation of the central stalk in F_1 where the rotation is converted into chemical energy. Electron microscopy of the V-type Na^+-ATPase of *C. fervidus* has demonstrated strong architectural similarities to F-type ATPases, which supports the view that V-type ATPases function according to a similar mechanism. A top view of the V_1 headpiece clearly shows the hetero hexameric complex of alternating A and B subunits (Boekema *et al*., 1998). Side views of the complex embedded in the membrane of small liposomes or in detergent solution showed the V_1 headpiece connected to the membrane embedded V_0 by a central stalk that is somewhat longer than in the F-type ATPases. In addition, a peripheral stalk was observed that is believed to be the ''stator'' that prevents idle rotation of V_1 relative to V_0 (Boekema *et al*., 1997). The peripheral stalk was visualized for the first time in the V-type Na^+-ATPase of *C. fervidus*, and has since also been demonstrated for F-type ATP synthases (Karrasch & Walker, 1999; Wilkens & Capaldi, 1998a,b; Böttcher *et al*., 1998).

The evolutionary relationship between the F and V-type ATPases/synthases is clear from the homology between the major subunits that constitute the headpiece and membrane-embedded parts. The nucleotide binding subunits of F_1, α and β, are homologous to the V_1 subunits B and A, respectively, while the F_0 subunit c that makes the rotor is homologous to subunit K in the *E. hirae* enzyme and the Vma3p, Vma11p and Vma16p subunits in the yeast vacuolar enzyme. On the other hand, the identification of the V-type subunits that correspond to the F_1 subunits γ, δ and ε and the F_0 subunits a and b is ambiguous (for instance, see Hunt & Bowman, 1997; Tomashek *et al*., 1997). Studies of the bacterial enzymes of *E. hirae* and *T. thermophilus* have identified subunits that are part of the soluble V_1 part of the complexes (Kakinuma & Igarashi, 1994; Yokoyama *et al*., 1994). Here, we present the complete subunit composition of the Na^+-ATPase of *C. fervidus* and show which of the subunits are part of V_1 and V_0. Analysis of more than 7500 electron micrograph images obtained from the enzyme complex in detergent solution reveals a much more detailed picture of the stator structure that connects the V_1 and V_0 parts (see also Boekema *et al*., 1999). The distribution of the subunits over V_1 and V_0 will be discussed in the context of a new structural model of the ATPase.

Results

Improved isolation of the V-ATPase

Previous studies of the Na^+-ATPase of *C. fervidus* were hampered by the difficulties in growing the strictly anaerobic, thermophilic organism to reasonable cell densities in large volumes and, consequently, in obtaining sufficient amounts of the purified ATPase complex. The optimized culturing procedure described in Materials and Methods resulted in exponential growth up to absorbancies of 1.2, measured at 660 nm in a 12.5 l fermentor. Moreover, a modified purification procedure resulted in a specific ATPase activity of the purified enzyme between 5-10 μmol/minute which was one to two orders of magnitude higher than before (Höner zu Bentrup *et al*., 1997). The procedure routinely yielded 0.75 mg of pure protein from a 12.5 l culture.

Subunit composition of the V-ATPase

The Na^+-ATPase of *C. fervidus* consists of nine subunits with apparent molecular masses determined by SDS-PAGE of 66, 61, 51, 37, 26, 25.5, 17, 12 and 10 kDa (Figure 1(a), lane 2). The 66 and 51 kDa subunits correspond to the catalytic subunits A and B of the V_1 part of the ATPase complex, respectively (Höner zu Bentrup *et al*., 1997). Heating the sample for five minutes at 80 °C before SDS-PAGE resulted in aggregation of the 61 and 17 kDa subunits as shown by the marked decrease in intensity of the corresponding bands and the appearance of stained material on top of the gel (lane 3). Such behavior is often observed for integral membrane proteins, suggesting that these subunits are part of the membrane-bound V_0. The 17 kDa subunit is typical for V-type ATPases and is the equivalent of the c subunit proteolipid of the F-type ATPases that forms the rotor in the V_0 part. Loading less protein or prolonged electrophoresis resolved the band running at 26 kDa in two separate bands of almost equal apparent molecular mass (Figure 1(b)). The two smaller subunits of 12 and 10 kDa had not been observed before (Höner zu Bentrup *et al*., 1997).

The sequence identity of the N-terminal sequences of the A and B subunit and the subunit composition suggest that the enzyme is very similar to the Na^+-ATPase of *E. hirae*, even though there are small differences in apparent molecular mass. We have assigned the *C. fervidus* subunits to the corresponding *E. hirae* subunits based on their apparent molecular mass and the intensities of the bands after Coomassie staining. Under the assumption that all subunits stain equally well with the dye, densitometric analysis of a Coomassie-stained gel containing the enzyme at three

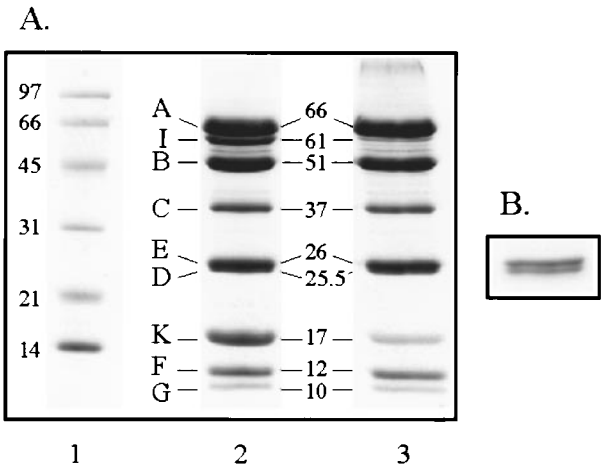

Figure 1. Subunit composition of the V_1V_0-ATPase of *C. fervidus*. (a) A SDS-12 % polyacrylamide gel was loaded with 20 µg of purified V_1V_0-ATPase and, after electrophoresis, stained with Coomassie. The samples were mixed with loading buffer and left at room temperature (lane 2) or heated for five minutes at 80 °C (lane 3) before loading onto the gel. Lane 1 shows the molecular mass markers. (b) A gel was loaded with 7.5 µg of purified V_1V_0 to show that the band at 26 kDa consists of two proteins with slightly different apparent molecular masses.

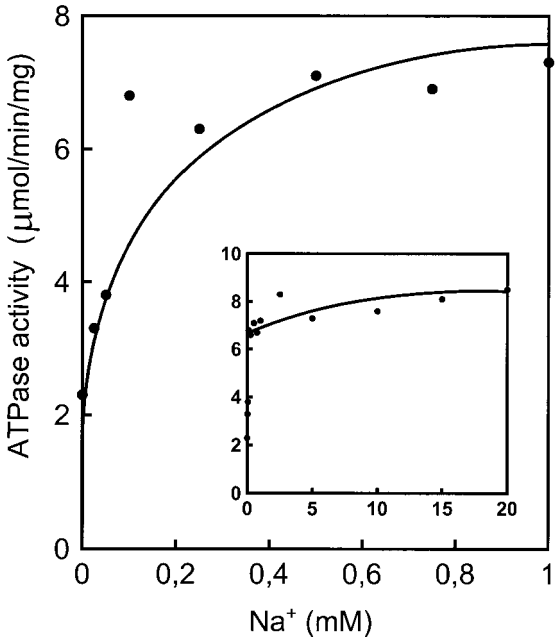

Figure 2. Na^+-dependent ATPase activity. The ATPase activity of the purified V_1V_0-ATPase was measured at increasing concentrations of Na^+ in 50 mM Mes (pH 6), 2 mM $MgCl_2$, 3 % glycerol and 0.05 % Triton X100, and at 50 °C. The main plot shows the ATPase activity in the Na^+ concentration range up to 1 mM, while the inset shows the activity in the concentration range up to 20 mM.

different amounts in a ratio of 1:3:9 suggested the following copy numbers of the subunits in the complex: A_3:I_2:B_3:C_1:$E_{2\text{-}3}$:D_1:K_5:$F_{2\text{-}3}$:G_1 (data not shown). The apparent molecular mass of the enzyme complex would be 700-750 kDa.

Na^+-dependent ATPase activity of the purified V-ATPase enzyme complex

The ATP hydrolysis activity of the purified V-ATPase complex increased in the presence of Na^+ in the assay buffer, but Na^+ was not required for a basal level of ATPase activity (Figure 2). The maximal stimulation of the hydrolysis rate by saturating concentrations of Na^+ varied between 3.5 and eight times for different enzyme preparations, suggesting a varying population of enzyme complexes in which the coupling between ATP hydrolysis and Na^+ translocation is lost. The concentration of Na^+ resulting in half the maximal stimulation was about 200 µM. The thermostability of the solubilized enzyme was measured by incubating the purified enzyme complex at elevated temperatures and measuring the residual ATPase activity in the presence and absence of Na^+. No loss of Na^+-independent ATPase activity was observed when the enzyme was incubated for one hour at 50 °C (Figure 3, filled squares). Prolonged incubation at 50 °C revealed a half-time of inactivation of about 24 hours (data not shown). In contrast, Na^+-dependent ATPase activity was rapidly inactivated at 50 °C. The activity dropped to the level of Na^+-independent ATPase activity in one hour (Figure 3, filled circles). The inactivation rate was clearly temperature-dependent because incubation at 40 °C resulted in a loss of only 10-20 % of the activity in one hour (Figure 2, filled triangles). At higher temperatures, the Na^+-dependency of the ATPase activity was lost more rapidly (data not shown). The data suggest that incubation of the enzyme complex at elevated temperature results in conversion from a Na^+-dependent to a Na^+-independent state of the enzyme. The optimum temperature of ATPase activity measured in the absence of Na^+ was about 70 °C, which corresponds to the temperature optimum for growth of *C. fervidus* (Figure 4, filled circles). Measurement of the temperature optimum of ATPase activity in the presence of Na^+ was troubled by the rapid inactivation at high temperatures. When assayed over the first 20 seconds, the optimum for Na^+-dependent ATPase activity was about 60 °C. Both the optimum and the maximal rate of ATP hydrolysis are likely to be underestimated because of the inactivation at higher temperatures.

Dissociation of the V-ATPase complex

The state of the V-ATPase enzyme complex upon incubation at elevated temperatures was ana-

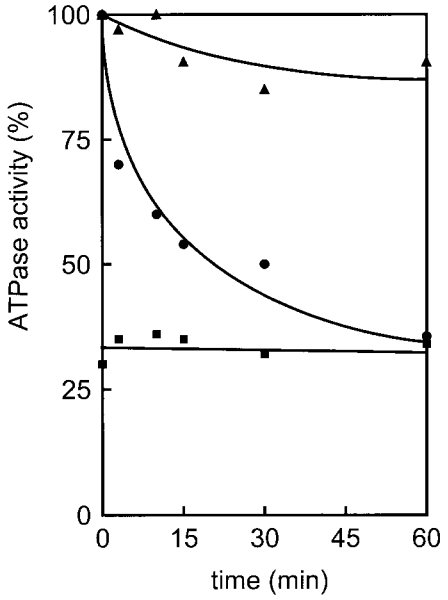

Figure 3. Thermostability. Residual ATPase activity of the purified V_1V_0-ATPase after incubation for the indicated times in the absence of Na^+ at 40 °C (▲) and 50 °C (●, ■). Residual ATPase activity was measured in the presence of 20 mM Na^+ (▲, ●) and without added Na^+ (■).

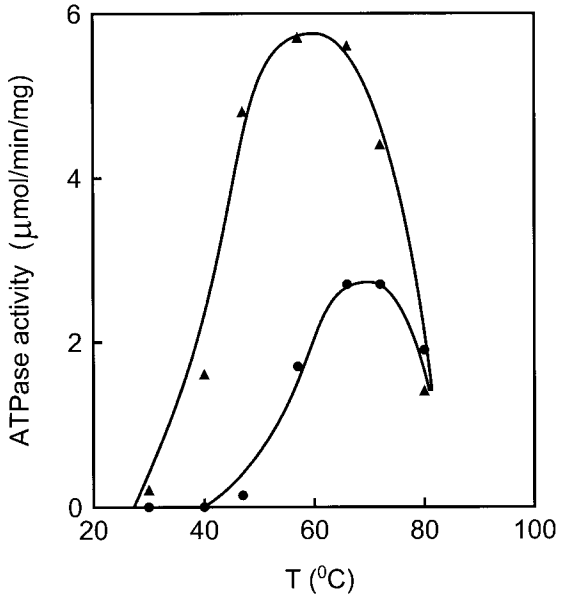

Figure 4. Temperature optimum. The ATPase activity of the purified V_1V_0-ATPase was measured at different temperatures in the presence (▲) and absence (●) of 20 mM NaCl in 50 mM Mes (pH 6), 2 mM $MgCl_2$, 3 % glycerol and 0.05 % Triton X100.

lyzed by native gel electrophoresis of the complex followed by activity staining. The purified V-ATPase complex had a very low mobility in a 3.8 % acrylamide gel (Figure 5(a), lane 1). Preincubation of the complex for 30 minutes at 50 °C before PAGE resulted in an active complex (complex I) of slightly higher mobility, and in the appearance of two new complexes, complexes II and III, that were active in ATP hydrolysis and which had much higher mobilities (lane 2). The latter two complexes were also present at low intensities in the original enzyme preparation. Staining the gel for protein with Coomassie revealed a significantly higher specific activity of complex III than observed for complex II. After two hours of preincubation, complex I had disappeared, while

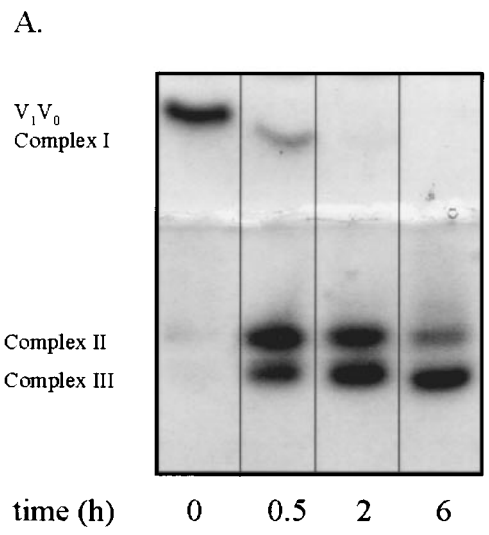

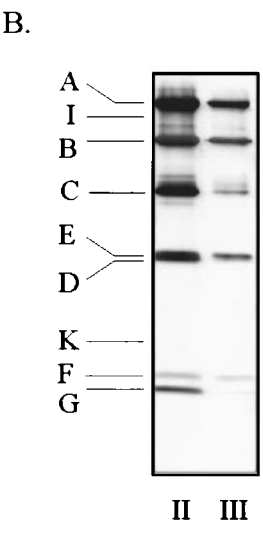

Figure 5. Dissociation of the V_1V_0-ATPase complex. (a) Native gel electrophoresis. The purified V_1V_0-ATPase was incubated at 50 °C in the absence of Na^+ at a protein concentration of 2.5 µg/µl for the indicated time, followed by native gel electrophoresis and activity staining. Lane 1 contains 15 µg of protein and lanes 2,3 and 4, 30 µg. (b) SDS-10 % PAGE of complexes II (left lane) and III (right lane). The activity stained bands representing complexes II and III were cut out of the native gel, cut in pieces, mixed with 40 µl of SDS loading buffer and incubated over night under continuous shaking. The gel was loaded with 25 µl samples and, after electrophoresis, stained with silver.

complexes II and III were decreased and increased in intensity, respectively (lane 3). Longer incubation resulted in a further decrease of complex II with a concomitant increase in complex III (lane 4). The experiments suggests that incubation of the enzyme complex at higher temperatures first results in a state with a slightly higher mobility (complex I) that subsequently is converted into complex II, which is then converted into complex III. The conversion of the enzyme into the latter two complexes correlates with the conversion of the Na^+-dependent into the Na^+-independent ATP hydrolysis activity of the complex (Figure 3).

Complexes I, II and III were cut out of the native gel and their subunit composition was analyzed by denaturing SDS-PAGE stained with silver. Complex I had the same subunit composition with the same relative staining intensities as the original enzyme preparation (data not shown), i.e. the increased mobility was not due to the loss of subunits. Complex II had lost the two subunits that were assigned to the V_0 part above: K and I (Figure 5(b), lane II). Prolonged electrophoresis showed that both subunits E and D were present in the same relative staining intensities as observed in the original enzyme complex. Apparently, the seven subunits A, B, C, E, D, F and G form a more or less stable complex that is active in ATP hydrolysis. In complex III, three additional subunits are lost, C, D and G (Figure 5(b), lane III). The small amount of subunit C still present (compare the relative intensities of subunits C and B in complexes II and III) most likely originates from carry over between the bands when they were cut out of the native gel. Subunits A, B, E and F constitute the next more or less stable, active complex that is formed from complex II upon incubation at higher temperatures.

Electron microscopy analysis

A total of 7561 side view projections were selected from electron micrographs of the purified ATPase enzyme complex in detergent solution. Classification of the data set in 64 classes (see Materials and Methods) revealed that the projections could be grouped in six predominant views, representing 56 % of the selected projections. These predominant views originate from substantially different orientations of the molecules on the carbon support film, as judged from the shape and features of the V_1 headpieces (see below). Most classes of the remaining 46 % of the projections were ''fuzzy'' average projections or represented wrongly aligned projections, projections with partially detached V_0 parts or with a strong kink between V_0 and V_1. These projections are not further discussed here. The 4258 projections of the six predominant views were redistributed into six groups and each group was further analyzed separately, as well as in combination with other groups. Significant additional variation was only present in the features of the stalk region of two of the six groups, resulting in the nine main projections shown in Figure 6.

All projections reveal the tripartite structure typical to V-type (and F-type) ATPases: the headpiece (V_1), membrane-embedded part (V_0), and a connecting stalk region. There are two types of headpiece views, a bilobed view (Figure 6(a)-(e)) and a trilobed view (Figure 6(f)-(i)). The bilobed view has an asymmetrical protruding density at the left or right sides (see the black arrow in Figure 6(e) and (a)-(c), respectively). In contrast, the trilobed view is much more symmetrical. Corresponding with the two views is the angle that the central stalk, that connects the V_1 and V_0 parts, makes with the vertical axis of the headpiece. In the bilobed views, the central stalk makes an angle of about 30°, while in the trilobed projections the central stalk coincides with the vertical axis. These features confirm observations made before with EM studies of the V-ATPase embedded in small liposomes (Boekema *et al*., 1998). In four of the six groups, a substantial part of the projections showed two peripheral stalks in addition to the central stalk (A, D, F, H). In the other two groups, these features were present at a frequency of no more than 5-10 % (data not shown). The two peripheral stalks are connected by a structure that is positioned just above the V_0 part and that seems to contact the central stalk. At this level, the distance of the two peripheral stalks to the central stalk is more or less similar in the bilobed views (Figure 6(a) and (d)), but significantly different in the trilobed views (Figure 6(f) and (h)). The peripheral stalks go all the way up to the top of V_1. They show up as an additional mass on top of the image when most of the stalk overlaps with V_1 (e.g. Figure 6(f) and (h)). The V_0 part has additional mass positioned asymmetrically at either the left (Figure 6(b), (e) and (i)) or right (Figure 6(a), (b), (f), (g) and (h)) side of the images (see white arrows in Figure 6(b), (f), (h) and (i)). The additional mass is connected to one of the peripheral stalks. In all cases where there is a clear connection between one of the peripheral stalks to V_0, the connection is at the side of V_0 where the additional mass is found (Figure 6(a), (b), (f), (g), (h) and (i)). The second peripheral stalk does not seem to be directly connected to the membrane embedded part.

Discussion

The V-type Na^+-ATPase of *C. fervidus* is similar to the Na^+-ATPase found in *E. hirae*. The genes coding for the nine subunits that constitute the latter enzyme complex are organized in the *ntp* operon that contains a total of 11 genes, *ntpFIKECGABDHJ*. The *ntpH* and *ntpJ* genes do not code for components of the ATPase complex (reviewed by Kakinuma, 1998). The *C. fervidus* enzyme also contains nine subunits. SDS-PAGE of the active protein complex cut from the gel after native gel

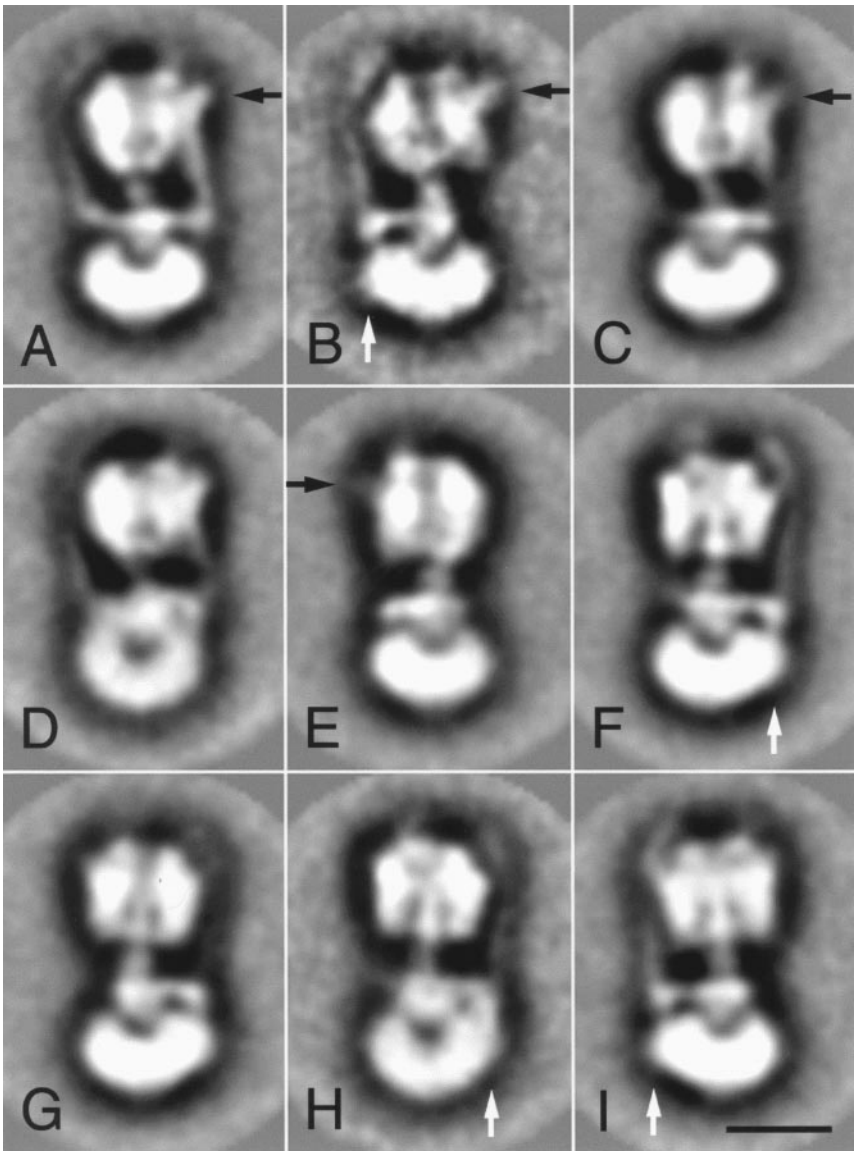

Figure 6. Analysis of side view projections of the V-ATPase. Images (a)-(i) show the six predominant views found by multivariate statistical analysis and classification of 7561 electron microscopy projections and the variation in the stalk region within these groups. (a), (b), (c) Averages from group 1, bilobed views in a position with flip-type handedness (1087 projections) with (a) two peripheral stalks (366 projections), with (b) the right peripheral stalk reduced (107 projections) and with (c) the left peripheral stalk reduced (424 projections). (d) Average of 321 out of the 509 projections of group 2, flip-type bilobed views with a reduced gap between V_0 and V_1. (e) Average of 384 out of the 582 projections of group 3, flop-type bilobed views. (f), (g) Averages from group 4, flip-type trilobed views (930 projections) with two peripheral stalks (577 projections) and with (g) both stalks reduced (344 projections). (h) Average of 253 out of the 651 projections of group 5, flip-type trilobed view with overlap between stalk region and V_0 part. (i). Average of 263 out of the 499 projections of group 6, flop-type trilobed views. For further explanation, see the text. The filled arrows in (a), (b), (c) and (e) pointing at the headpiece indicate the ''asymmetrically protruding densities'' (see the text). The open arrows in (b), (f), (h) and (i) pointing at the V_0 parts indicate the ''asymmetrically positioned densities'' (see the text). The bar represents 10 nm.

electrophoresis of the purified V_1V_0 revealed subunits with molecular masses of 66, 61, 51, 37, 26, 25.5, 17, 12 and 10 kDa. In all preparations, the two subunits with molecular masses of 26 and 25.5 kDa were present at the same intensity ratio, indicating that these represent two separate subunits. Moreover, a complex was isolated (complex III) that still contained the 26 kDa subunit, but lacked the 25.5 kDa subunit (see below). Previously, we showed a high similarity of the N-terminal sequences of the 66 and 51 kDa subunits with the *E. hirae* A and B subunits, respectively (Höner zu Bentrup *et al.*, 1997). Based on the apparent molecular mass and relative staining intensities with Coomassie after SDS-PAGE we could assign the other subunits of the *C. fervidus* enzyme. The I, C and K subunits were easily identified because of very similar molecular masses and corresponding intensities. The *E. hirae* subunit D (27 kDa) has a higher apparent molecular mass than subunit E (24 kDa), but is present in lower copy number. Therefore, we assigned the 26 kDa band of *C. fervidus* to subunit E and the 25.5 kDa band to subunit D. Subunit F of *C. fervidus* has a lower apparent molecular mass than subunit K, the proteolipid, while this is the other way around in *E. hirae*. The smallest subunit G is 10 kDa in *C. fervidus* and 8 kDa in *E. hirae* (see Figure 1).

The A and B subunits are the major V_1 subunits that form the hetero-hexameric headpiece that consists of three A and three B subunits. (Boekema *et al.*, 1998). Subunit K is the equivalent of the F-type subunit c, the major membrane bound subunit that is believed to be present in 9-12 copies. Subunit K is twice as large as the c subunit and the product of a gene duplication. Densitometric anal-

ysis after Coomassie staining suggested five copies of subunit K in the complex. Subunit I does not have a counterpart in F-type ATPases. The *E. hirae ntpI* gene product consists of a soluble N-terminal half and a typical membrane-bound C-terminal half. Subunit I may combine the functions of the subunits a and b of F-type ATPases. The latter consists of a small membrane-bound part and a soluble part that is thought to be part of the stator structure. Remarkably, both the *C. fervidus* and *E. hirae* data suggest two copies of I per complex, while only one copy of the a subunit is present in the F-type ATPases. The other five subunits C, D, E, F, G are hydrophilic in nature, but their function is unknown. Subunits C, D and G are present in a single copy, while subunits E and F are present in multiple copies. The estimates from the *C. fervidus* enzyme are consistently higher (two to three copies) than the estimates from the *E. hirae* enzyme (one or two copies).

Subunits other than A and B of V_1, and K and I of V_0 have been assigned to either V_1 or V_0 by dissociating the enzyme complex. Chloroform extraction of membranes containing the V-type ATPase of *T. thermophilus* resulted in a soluble complex of four subunits with apparent molecular masses of 66 (A), 55 (B), 30 and 11 kDa (Yokoyama *et al.*, 1990). EDTA extraction of *E. hirae* membranes released a complex that, besides the A and B subunits, contained the C, D, E and F subunits (Kakinuma, 1998). Here, the V-ATPase complex of *C. fervidus* was dissociated by heating the enzyme in detergent solution at 50 °C. A complex was formed (complex II) that was active in ATP hydrolysis activity. The formation of the complex seemed to correlate with the loss of Na^+-dependent ATP hydrolysis, suggesting a loss of the coupling between V_1 and V_0. Analysis of the subunit composition of complex II revealed the loss of the two V_0 subunits, K and I and, consequently, showed that subunits C, D, E, F and G form a complex with the catalytic subunits A and B. We tentatively conclude that complex II corresponds to V_1, even though it cannot be excluded that either of subunits C, D, E, F and G are membrane-bound. In the latter case they would only weakly interact with the other V_0 subunits. In the next step, the subunits that are present in a single copy, C, D, and G dissociate from the complex, yielding complex III, indicating that these are loosely bound. This may explain the absence of the G subunit in the EDTA extracted complex of the *E. hirae* enzyme. Subunits E and F are only lost upon prolonged incubation, leaving the A and B subunit core of the headpiece that has been visualized in top view by electron microscopy (Boekema *et al.*, 1998). The temperature driven dissociation of the V-ATPase of *C. fervidus* is schematically indicated in Figure 7.

A previous electron microscopy study of the V-ATPase of *C. fervidus*, involving the averaging of relatively few single particles in side view projection, showed besides the central stalk that connects

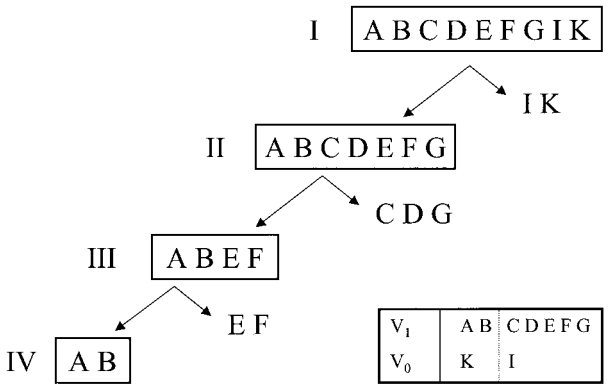

Figure 7. Temperature driven disassembly of the V_1V_0-ATPase. See the text for an explanation.

V_1 and V_0, a peripheral stalk, termed the stator (Boekema *et al.*, 1997, 1998). The stator would be responsible for fixing the static part of V_0 relative to V_1 in the rotary catalysis mechanism. The present series of side view averages indicates that the stator structure is more complicated and consists of at least two peripheral stalks. Figure 8 gives an analysis of two trilobed (a) and (b)) and the two bilobed ((c) and (d)) side view projections and how they relate to one another. The tri- and bilobed views of the headpiece are a consequence of different orientations of the molecules on the grid (see the top views). In the trilobed views, one A and one B subunit are in the center of the particle in projection, resulting in a symmetrical view with stain accumulating in the two grooves flanking the central subunit. In the bilobed views, the molecules are rotated by 30° along the long axis of the molecule. Central in the projection is a groove in between the A and B subunits and, importantly, because of the different molecular masses of the A and B subunits, the mass distribution is asymmetrical. The two peripheral stalks are clearly visible in the trilobed view in Figure 8(a) and the bilobed view in Figure 8(c). In the trilobed view, in projection, the left stalk is positioned significantly closer to the central stalk than the right stalk. In the bilobed view the distance is more or less the same, even though the angle with the central stalk is clearly different. Both projections are in agreement with the side stalks placed in the groove in between the A and B subunits (open circles in the top views) rather than as radial extensions of either the A or B subunits. We cannot exclude the possibility that there are three peripheral stalks, in line with the 3-fold symmetry in the AB hexamer. In projection, the third stalk would be at the same position as one of the other two stalks. For instance, in Figure 8(a), the third stalk would coincide with the left stalk. Arguing against the possibility of a third peripheral stalk is that we do

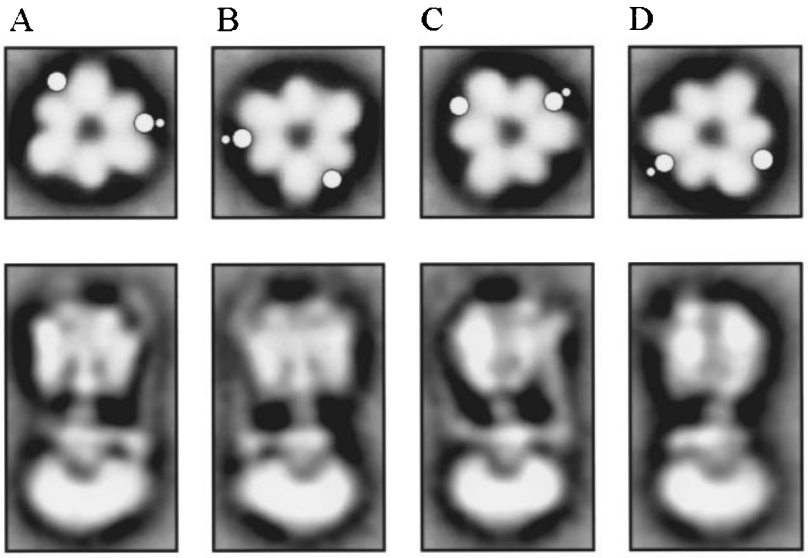

Figure 8. Relative orientation of four groups of side view projections of the V-ATPase. Possible relation between four side view projections (below) indicated by the top view projections (above). The side view projections are a selection taken from Figure 6 ((f), (i), (a) and (e): from left to right). The top view was as described by Boekema *et al.*, (1998). The open circles in the top views represent the position of the two peripheral stalks; the small open circles indicate the attachment site of one of the peripheral stalks to V_0. The arrow on the right indicates the direction of projection that results in the side view projections.

not see the density at this position in the projection twice. Therefore, we conclude that there could be a third peripheral stalk although none of the projections shows any evidence for this.

One of the peripheral stalks appears to be connected to the membrane-bound part, which introduces asymmetry in both the stalk and V_0 region (indicated by a small circle in the top views). This stalk is connected, to additional mass that is present at either the right (Figure 8(a) and (c)) or left (Figure 8(b) and (d)) side of V_0. In projection, the two peripheral stalks are connected by a bar that is positioned just above V_0, parallel to the plane of the membrane. In conclusion, side view projection (a) and (b), and (c) and (d) relate to one another through 180° rotations and side view (c) is obtained from side view (a) by a 30° counter clockwise rotation. The positions of the stators as deduced from the side views, cannot be directly verified from top view projections, since such projection are not present in significant numbers if intact V_0V_1 molecules are prepared. However, in a recent report on top view projections of *Manduca sexta* V_1-ATPase, a small density is clearly visible in the groove between the A and B subunits, in agreement with our modelling (Radermacher *et al.*, 1999). No clear indication for a second density that would correspond to the second peripheral stalk was found in this study.

Figure 9 represents a hypothetical model of the V-ATPase of *C. fervidus* that is based on the present studies. Subunits A and B form the headpiece and subunit K the rotor of the membrane-embedded part. The asymmetric density observed in V_0 is formed by the hydrophobic C-terminal half's of two copies of subunit I. The hydrophilic N-terminal half's of the I subunits emerge from the membrane and may go up along the side of V_1 to form the peripheral stalk that is connected to V_0. Alternatively, they may form (part of) the bar that connects the two peripheral stalks. This bar may function in addition as a bearing for the central stalk that fixes the distance between the static and dynamic parts of V_0 at which interface the Na^+ are translocated. At this moment, it is not possible to assign the other subunits in the model. Currently,

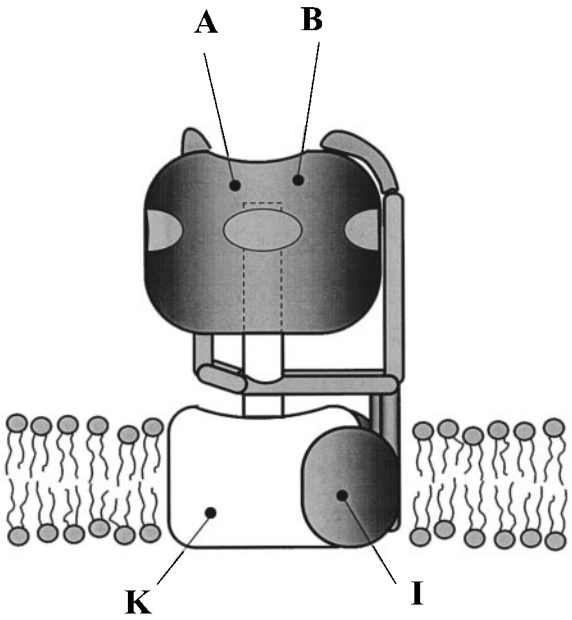

Figure 9. The V_0V_1-ATPase of *C. fervidus* based on the present studies. The rotor of V_0 (subunits K) and the central stalk rotate relative to the static shaded parts.

we are working on the purification of complexes II and III and plan to study their structure by EM to refine the model.

Materials and Methods

Growth conditions and membrane preparation

C. fervidus ATCC 43024 was grown anaerobically at 60 °C in trypton-yeast extract-glucose medium, pH 7 (Patel *et al*., 1987) containing 2 mM Na_2S following a three-step procedure. In the first step, 10 ml of medium in a 100 ml serum bottle was inoculated with a glycerol stock of cells kept at −80 °C and the culture was grown until an absorbancy, measured at 660 nm of 0.5 was attained. Subsequently, the culture was diluted tenfold in a one liter serum bottle and, again, grown until an absorbancy of 0.5 was reached. The cultures were not stirred and anaerobic conditions were monitored through the presence of resazurin in the medium at a concentration of 100 µg/l. The one liter culture was used in the third and final step to inoculate 12.5 l of medium in a 15 l fermentor. The pH in the fermentor was kept constant by titration with an anaerobic KOH solution and the culture was stirred intermittently. Cells were harvested at an absorbancy of 1-1.2 in the late exponential growth phase, washed once and resuspended in 50 mM *N*-2-morpholinepropane-sulfonic acid (Mops (pH 7) containing 5 mM $MgCl_2$. No specific precautions were taken to keep the cells anaerobic after growth. The yield was typically 30 g of cells (wet-mass) and the cells were stored in liquid nitrogen.

Cells from a 12.5 1 culture were disrupted in a French Press operated at 20,000 psi at 4 °C in the presence of 5 mM dithiothreitol (DTT), 1 mM phenylmethylsulfonylfluoride (PMSF) and trace amounts of DNAase and RNase. Unbroken cells and debris were removed by centrifugation for ten minutes at 10,000 *g* after which the membranes were collected by centrifugation for one hour at 200,000 *g* in a Beckman ultracentrifuge. The membranes were resuspended in 50 mM Mops (pH 7), 5 mM $MgCl_2$ at a concentration of 20 mg/ml and stored in liquid nitrogen.

Purification of the Na^+ATPase

Membranes were resuspended in a final volume of 12 ml buffer 50 mM Mops (pH 7), 5 mM $MgCl_2$, 3 % (w/v) glycerol, 5 mM DTT containing 50 mM KCl at a concentration of 10 mg/ml. Triton X100 was added to the suspension from a stock of 20 % (v/v), yielding a final concentration of 3 % Triton X100, followed by gentle agitation for 20 minutes at room temperature. Undissolved material was removed by ultracentrifugation for 20 minutes at 350,000 *g* at 4 °C. The supernatant was diluted threefold with buffer A containing 75 mM KCl to reduce the Triton X100 concentration to 1 %. The sample was loaded on a DEAE column (2.5 cm × 1.5 cm (W × H) bed size), preequilibrated in buffer A containing 75 mM KCl and 0.5 % Triton X100. The DTT concentration was reduced to 2 mM. The column was washed with 20 ml of the equilibration buffer and 10 ml with the same buffer containing 0.1 % rather than 0.5 % Triton X100. The column, run at room temperature, was eluted batchwise with 20 ml of buffer A containing 150 mM KCl and 0.1 % Triton X100. During the whole procedure, fractions of 2 ml were collected and samples of 5 µl were assayed for ATPase activity. Active fractions were pooled (typically 6-8 ml) and concentrated to 1 ml by ultrafiltration using Biomax-100k filters (Millipore). The concentrated sample was loaded on a HiLoad 26/60 Superdex 200 size-exclusion column equilibrated in buffer A containing 50 mM KCl and 0.05 % Triton X100. The column was run in the cold room at 1 ml/minute and fractions of 1.8 ml were collected and assayed for ATPase activity. The enzyme complex that eluted in the void volume of the column was concentrated by ultrafiltration and stored in liquid nitrogen. Protein concentration was measured according to Bradford using bovine serum albumin as a standard.

ATPase activity assay

ATP hydrolysis was estimated from the amount of P_i released as measured with malachite green molybdate reagent. Routinely, ATPase activity in the column fractions obtained during the purification procedure was determined using microtiter plates as described by Höner zu Bentrup *et al*. (1997). The absorbancy of the samples in the micro titer plates was read at 660 nm in a SpectraMax 320 spectrophotometer (Molecular Devices, Inc).

For the characterization of the purified enzyme, a different assay was used because of the thermo-instability of the complex at higher temperatures (see the Results). A volume of 31 µl of ATPase buffer containing 50 mM Mes (pH 6), 2 mM $MgCl_2$, 3 % glycerol and 0.05 % Triton X100, and 20 mM NaCl when indicated was equilibrated at the indicated temperature, after which 2 µl of 35 mM Tris-ATP was added, followed at 15 seconds by an aliquot of 2 µl of the purified enzyme complex. The reaction was allowed to proceed for 20 seconds and stopped by freezing the tube in liquid nitrogen. The sample was thawed on ice, spun briefly to collect the contents at the bottom of the tube, and a sample of 30 µl was mixed with 200 µl of the malachite green solution in a microtiter plate. After three minutes the absorbancy was measured at 660 nm.

Polyacrylamide gel electrophoresis

Native gel electrophoresis was based on a method described by Schägger & Jagow (1991). The gel consisted of three parts containing 3.5, 3.8 and 8 % of acrylamide at a ratio of 2:3:7. The anode buffer contained 50 mM Bis-Tris-propane, adjusted to pH 7 with concentrated HCl, the cathode buffer contained 50 mM Mes, adjusted to pH 7 using Bis-Tris-propane, and 0.1 % Triton X-100. The samples were gently mixed with sample buffer (5 % Triton X-100, 50 % glycerol, 0.5 M Mes (pH 7), 0.5 % bromphenol blue). The gel was run at a constant current of 25 mA for four hours. For ATPase activity staining, the top part of the gel (3.5 % acrylamide) was removed, after which the gel was incubated for 20 minutes at 45 °C in ATPase assay buffer supplemented with 50 mM NaCl and 3 mM Tris-ATP. Liberated P_i was made visible by staining the gel for five minutes with malachite green molybdate reagent before fixation in 34 % (w/v) citric acid.

Electron microscopy

Freshly purified V-ATPase was concentrated to 1.5 mg/ml by ultrafiltration and prepared for EM by

diluting about 500-fold with 5 mM Mops buffer containing 0.05% Triton X100 using the droplet method with 2% uranyl acetate as negative stain. Micrographs were recorded with a Philips CM10 electron microscope at 52,000 × magnification. A total of 7561 projections were extracted from 96 electron micrographs, digitized with a Kodak Eikonix model 1412 CCD camera and analyzed with IMAGIC software (Harauz *et al.*, 1988). Images were band-pass filtered and normalized, and subsequently subjected to multireference alignment, multivariate statistical analysis and classification. In the final summing of class members, variable numbers of projections were summed to optimize the balance between signal-to-noise ratio and visibility of the stator features, using the cross-correlation coefficient from the alignment step as the objective quality parameter for summing.

References

Abrahams, J. P., Leslie, A. G., Lutter, R. & Walker, J. E. (1994). Structure at 2.8 Å resolution of F1-ATPase from bovine heart mitochondria. *Nature,* **370**, 621-628.

Boekema, E. J., Ubbink-Kok, T., Lolkema, J. S., Brisson, A. & Konings, W. N. (1997). Visualization of a peripheral stalk in V-type ATPase: evidence for the stator structure essential to rotational catalysis. *Proc. Natl Acad. Sci. USA,* **94**, 14291-14293.

Boekema, E. J., Ubbink-Kok, T., Lolkema, J. S., Brisson, A. & Konings, W. N. (1998b). Structure of V-type ATPase from *Clostridium fervidus* by electron microscopy. *Photosynthesis Res.* **57**, 267-273.

Boekema, E. J., van Breemen, J. F. L., Brisson, A., Ubbink-Kok, T., Konings, W. N. & Lolkema, J. S. (1999). Biological motors: connecting stalks in V-type ATPase. *Nature,* **401**, 37-38.

Böttcher, B., Schwarz, L. & Graber, P. (1998). Direct indication for the existence of a double stalk in CF_0F_1. *J. Mol. Biol.* **281**, 757-762.

Boyer, P. D. (1993). The binding change mechanism for ATP synthase-some probabilities and possibilities. *Biochim. Biophys. Acta,* **1140**, 215-250.

Collins, M. D., Lawson, P. A., Willems, A., Cordoba, J. J., Garcia, J., Fernandez-Garayzabal, P., Cai, J., Hippe, H. & Farrow, J. A. E. (1994). The phylogeny of the genus *Clostridium*: proposal of five new genera and eleven new species combinations. *Int. J. Syst. Bacteriol.* **44**, 812-826.

Harauz, G., Boekema, E. J. & van Heel, M. (1988). Statistical image analysis of electron micrographs of ribosomal subunits. *Methods Enzymol.* **164**, 35-49.

Höner zu Bentrup, K., Ubbink-Kok, T., Lolkema, J. S. & Konings, W. N. (1997). An Na^+-pumping V_1V_0-ATPase complex in the thermophilic bacterium *Clostridium fervidus*. *J. Bacteriol.* **179**, 1274-1279.

Hunt, I. E. & Bowman, B. J. (1997). The intriguing evolution of the ''b'' and ''G'' subunits in F-type and V-type ATPases: isolation of the *vma*-10 gene from *Neurospora crassa*. *J. Bioenerg. Biomembr.* **29**, 533-540.

Kakinuma, Y. (1998). Inorganic cation transport and energy transduction in *Enterococcus hirae* and other streptococci. *Microbiol. Mol. Biol. Rev.* **62**, 1021-1045.

Kakinuma, Y. & Igarashi, K. (1995). Electrogenic Na^+ transport by *Enterococcus hirae* Na^+-ATPase. *FEBS Letters,* **359**, 255-258.

Kakinuma, Y. & Igarashi, K. (1994). Purification and characterization of the catalytic moiety of vacuolar-type Na(+)-ATPase from *Enterococcus hirae*. *J. Biochem.* **116**, 1302-1308.

Karrasch, S. & Walker, J. E. (1999). Novel features in the structure of bovine ATP synthase. *J. Mem. Biol.* **290**, 379-384.

Noji, H., Yasuda, R., Yoshida, M. & Kinosita, K. J. (1997). Direct observation of the rotation of F1-ATPase. *Nature,* **386**, 299-302.

Patel, B. K. C., Monk, C., Morgan, H. W. & Daniel, R. M. (1987). *Clostridium fervidus* sp. nov., a new chemoorganotrophic acetogenic thermophile. *Int. J. Syst. Bacteriol.* **37**, 123-126.

Sabbert, D., Engelbrecht, S. & Junge, W. (1996). Intersubunit rotation in active F-ATPase. *Nature,* **381**, 623-625.

Radermacher, M., Ruiz, T., Harvey, W. R., Wieczorek, H. & Grüber, G. (1999). Molecular architecture of *Manduca sexta* midget V_1 ATPase visualized by electron microscopy. *FEBS Letters,* **453**, 383-386.

Schägger, H. & von Jagow, G. (1991). Blue native electrophoresis for isolation of membrane protein complexes in enzymatically active form. *Anal. Biochem.* **199**, 223-231.

Speelmans, G., de Vrij, W. & Konings, W. N. (1989). Characterization of amino acid transport in membrane vesicles from the thermophilic fermentative bacterium *Clostridium fervidus*. *J. Bacteriol.* **171**, 3788-3795.

Speelmans, G., Poolman, B. & Konings, W. N. (1993a). Amino acid transport in the thermophilic anaerobe *Clostridium fervidus* is driven by an electrochemical sodium gradient. *J. Bacteriol.* **175**, 2060-2066.

Speelmans, G., Poolman, B., Abee, T. & Konings, W. N. (1993). Energy transduction in the thermophilic anaerobic bacterium *Clostridium fervidus* is exclusively coupled to sodium ions. *Proc. Natl Acad. Sci. USA,* **90**, 7975-7979.

Speelmans, G., Poolman, B., Abee, T. & Konings, W. N. (1994). The F- or V-type Na(+)-ATPase of the thermophilic bacterium *Clostridium fervidus*. *J. Bacteriol.* **176**, 5160-5162.

Takase, K., Yamato, I. & Kakinuma, Y. (1993). Cloning and sequencing of the genes coding for the A and B subunits of vacuolar-type Na(+)-ATPase from *Enterococcus hirae*. Coexistence of vacuolar- and F_0F_1-type ATPases in one bacterial cell. *J. Biol. Chem.* **268**, 11610-11616.

Takase, K., Kakinuma, S., Yamato, I., Konishi, K., Igarashi, K. & Kakinuma, Y. (1994). Sequencing and characterization of the ntp gene cluster for vacuolar-type Na(+)-translocating ATPase of *Enterococcus hirae*. *J. Biol. Chem.* **269**, 11037-11044.

Tomashek, J. J., Graham, L. A., Hutchins, M. U., Stevens, T. H. & Klionsky, D. J. (1997). V1-situated stalk subunits of the yeast vacuolar proton-translocating ATPase. *J. Biol. Chem.* **272**, 26787-26793.

Tsutsumi, S., Denda, K., Yokoyama, K., Oshima, T., Date, T. & Yoshida, M. (1991). Molecular cloning of genes encoding major two subunits of a eubacterial V-type ATPase from *Thermus thermophilus*. *Biochim. Biophys. Acta,* **1098**, 13-20.

Wilkens, S. & Capaldi, R. A. (1998a). Electron microscopic evidence of two stalks linking the F1 and F0 parts of the *Escherichia coli* ATP synthase. *Biochim. Biophys. Acta,* **1365**, 93-97.

Wilkens, S. & Capaldi, R. A. (1998b). ATP synthase's second stalk comes into focus. *Nature,* **393**, 29.

Yokoyama, K., Oshima, T. & Yoshida, M. (1990). *Thermus thermophilus* membrane-associated ATPase.

Indication of a eubacterial V-type ATPase. *J. Biol. Chem.* **265**, 21946-21950.

Yokoyama, K., Akabane, Y., Ishii, N. & Yoshida, M. (1994). Isolation of prokaryotic V_0V_1-ATPase from a thermophilic eubacterium *Thermus thermophilus*. *J. Biol. Chem.* **269**, 12248-12253.

Yokoyama, K., Muneyuki, E., Amano, T., Mizutani, S., Yoshida, M., Ishida, M. & Ohkuma, S. (1998). V-ATPase of *Thermus thermophilus* is inactivated during ATP hydrolysis but can synthesize ATP. *J. Biol. Chem.* **273**, 20504-20510.

Edited by W. Baumeister

(Received 16 September 1999; received in revised form 3 December 1999; accepted 8 December 1999)